Title: Methane-fed microbial communities enriched from field-grown rice support diverse heterotrophic bacteria

Running title: Methane-fed enrichments from rice

Authors: Elena K. Perry[a], Aqib Hasnain[a], Benjamin J. Cole[b], Hans K. Carlson[a], Adam M. Deutschbauer[a], Dawn Chiniquy[a#]

Author affiliations:

[a]Environmental Genomics and Systems Biology Division, Lawrence Berkeley National Laboratory, Berkeley, CA, USA

[b]DOE Joint Genome Institute, Lawrence Berkeley National Laboratory, Berkeley, CA, USA

[#]Correspondence: dmchiniquy@lbl.gov

Abstract

Rice paddies naturally host aerobic methanotrophic bacteria, due to the production of methane in flooded soils. However, relatively little is known about how the activity of methanotrophs impacts the structure of the broader microbial community in this globally important agricultural environment. To address this question, we passaged 51 aerobic microbial enrichment cultures from rice rhizosphere, root, and stem samples in a chemically-defined medium with methane as the primary carbon source and electron donor. We profiled the cultures over time by 16S rRNA gene amplicon sequencing and sequenced the genomes of 40 isolates from the enrichments to gain functional insights. Taxa whose relative abundance increased during community growth on methane represented more than a dozen families, many of which are not known to utilize methane or other one-carbon substrates. Despite the selective pressure imposed by the culture condition, the final community structures were taxonomically varied rather than converging to a common composition. Genomic analysis of the sequenced isolates revealed considerable variation in likely carbon source utilization repertoires, as well as the capacity for nitrogen fixation or denitrification. Taken together, these findings support the view that methanotrophy represents a key link in the microbial food web of rice fields, with the potential for downstream effects on the abundance and activity of a wide range of community members.

Importance

Rice paddies produce the primary staple food for more than half of the world's population, but are also a major source of methane emissions. Methane-oxidizing bacteria known as methanotrophs naturally occur in rice paddies, where they consume methane that would otherwise escape to the atmosphere. Enhancing the activity of native methanotrophs could improve the sustainability of rice cultivation. However, large gaps remain in our knowledge of how increased

methanotrophic activity could impact other members of rice paddy microbial communities, leaving open the possibility of unintended effects on other important microbial ecosystem functions, such as nitrogen cycling. This study sheds light on the taxonomic range and metabolic capacities of rice-associated bacteria that can benefit from the activity of native methanotrophs, laying the foundation for a broader understanding of how methanotrophs impact microbiome assembly and nutrient cycling in rice paddies.

Introduction

Microbes that oxidize one-carbon compounds, such as methane and methanol, play a key role in global nutrient cycles. In particular, aerobic methanotrophs in the phylum Pseudomonadota are the most widespread functional guild contributing to microbial methane oxidation. Aerobic methanotrophs are classically divided into two major groups, type I (Gammaproteobacteria) and type II (Alphaproteobacteria); type I methanotrophs use the ribulose monophosphate (RuMP) pathway for carbon assimilation into biomass, while type II use the serine pathway. Because these bacteria can use methane as a sole carbon and energy source, they are found in a variety of environments where methane is abundant, such as wetlands, freshwater lake sediments, and landfill cover soils (1). Besides contributing to carbon cycling via methane oxidation, methanotrophs may also play an important role in the global nitrogen cycle: many proteobacterial methanotrophs are capable of nitrogen fixation (2), although conversely, methanotrophs have also been shown to stimulate the activity of denitrifying bacteria (3, 4).

Consistent with the latter observation, it is thought that methanotrophs often interact metabolically with other members of their native microbial communities (5). Methanotrophs are notoriously difficult to isolate (6), and culturing methanotrophs in the presence of other heterotrophic bacteria frequently increases methane oxidation rates and overall biomass yields (7, 8). Such partnerships may benefit the methanotrophs by preventing the accumulation of inhibitory metabolic byproducts or providing essential vitamins (7, 9). Methanotrophs can in turn provide benefits to their neighbors. Studies using stable-isotope probing (SIP) have demonstrated that carbon derived from methane by methanotrophs in a variety of environments can end up in the biomass of diverse other organisms (10–15). Thus, methanotrophs contribute to local microbial food webs by transforming methane into other, more bioavailable carbon sources.

While the existence of metabolic exchanges between methanotrophs and other bacteria is well-established, relatively little is known about how methanotrophs influence the microbial communities of methane-rich wetland environments, including rice paddies (16). Recently, methanotrophs have been shown to stimulate both nitrogen fixation and denitrification in rice paddies, depending on the environmental conditions (12, 17), but the full range of their impact on the rice microbiome remains unclear. Given the roles of methanotrophs in both carbon and nitrogen cycling, an improved understanding of their ecological influence in rice paddies could have significant implications for improving the productivity and sustainability of rice cultivation. This issue is of global importance since rice is one of the world's most widely-consumed staple crops (18). The most concrete evidence that specific taxa might preferentially benefit from methane-derived carbon in rice fields has come from DNA-SIP studies on microcosms of paddy soils or rice roots (10, 12). In these studies, the bacteria that incorporated the ^{13}C label mainly belonged to the Alphaproteobacteria and Betaproteobacteria, although the results varied at lower taxonomic levels. However, the sensitivity of DNA-SIP is limited and the results can be significantly affected by experimental parameters such as incubation time (19), thus motivating the use of complementary approaches to determine the range of microbial taxa that may benefit from methanotrophic activity in rice fields.

Here, we performed 16S rRNA gene amplicon-based profiling on methane-fed enrichment cultures, complemented by whole-genome sequencing of strains isolated from the enrichments, to gain new insights into how methanotrophs from rice paddies influence their native communities. Specifically, we addressed the following questions: 1) What is the taxonomic diversity of rice-associated bacteria that can be supported by methane-derived carbon? 2) To what extent is the community composition of methane-fed enrichment cultures affected by external variables such

as the part of the rice plant used for the inoculum? 3) Is the impact of methanotrophs on the rice microbiome predictable, as indicated by recurring community assembly patterns (if any) during growth on methane as the sole exogenous carbon source? 4) What carbon sources are the most likely drivers of non-methanotrophic growth in methane-fed, methanotroph-anchored communities?

Results

Methane-fed enrichment cultures maintained high alpha diversity

We established 51 enrichment cultures in chemically-defined media with methane as the sole electron donor and oxygen as the major electron acceptor, inoculated with rice rhizosphere, root, and stem samples collected from two field locations in California, as described in Materials and Methods. The cultures were sampled weekly over 12 weeks for 16S rRNA gene amplicon-based profiling of community composition, resulting in a total of 534 sequenced samples (excluding those that failed to meet our threshold for minimum reads; see Materials and Methods); the complete amplicon sequence variant (ASV) abundance table and sample metadata are available in Tables S1 and S2, respectively. At the final time point, 16 families belonging to three phyla (Pseudomonadota, Bacteroidota, and Verrucomicrobiota) achieved a relative abundance of >10% in at least two enrichments (Fig. 1A). Two additional higher-level taxonomic groups, consisting of ASVs that could not be classified beyond the order Rhizobiales or the domain Bacteria, met the same criteria for abundance and prevalence. By far the most prominent families across the final enrichment communities, when considering both prevalence and relative abundance, were Comamonadaceae (>10% in 33/51 enrichments, mean relative abundance 16.3%) and Methylocystaceae (>10% in 29/51 enrichments, mean relative abundance 22.4%).

109 Comamonadaceae does not contain any known methanotrophs, but Methylocystaceae represents
110 the Type II methanotrophs. Type I methanotrophs, represented by the family Methylococcaceae,
111 were less prevalent in the final enrichments (>10% in 4/51 enrichments).

112 Interestingly, while all of the final enrichment communities contained a detectable level of
113 at least one putative methanotroph ASV classified as Methylocystaceae or Methylococcaceae,
114 methanotrophs were not always the most abundant community members. Methanotrophs
115 represented the majority of reads in just eight out of the 51 final communities. In 16 out of the 51
116 enrichments (nearly 1/3) the final total methanotroph relative abundance was <10%, and the lowest
117 final total methanotroph relative abundance was just 0.2%. Inspecting the relative abundances of
118 putative methanotroph ASVs over time revealed that in many of the enrichments, methanotroph
119 abundances fluctuated or dropped after reaching a peak prior to the final time point, rather than
120 steadily increasing over time—especially for many of the Type I methanotrophs (Fig. 1B).
121 Additionally, in most of the enrichments only one or two methanotroph ASVs were abundant at
122 any given time (Fig. 1B-C). By contrast, individual enrichments supported up to 80 non-
123 methanotroph ASVs (with a median of 39) at the final time point (Fig. 1C).

124 We also assessed how overall alpha diversity was affected by time, sample type, and initial
125 inoculum dilution. For rhizosphere and root enrichments, the number of ASVs observed per
126 enrichment initially dropped noticeably compared to the inoculum, but subsequently fluctuated
127 around the value reached by the end of week one, rather than continuing to decline, despite the
128 1:10 dilution transfers that were performed after week four and week eight (Fig. 1D). For stem
129 enrichments, the number of observed ASVs dropped only slightly in the first week, and fluctuated
130 around the original value thereafter (Fig. 1D). Community evenness followed generally similar
131 patterns over time for the different sample types (Fig. 1E). At the final time point, the number of

132 observed ASVs was significantly lower for stem enrichments compared to rhizosphere and root
133 enrichments, but did not differ between the latter two groups (Fig. 1F). Initial inoculum dilution
134 had no statistically significant effect on the final number of observed ASVs (Fig. 1G).

135 *Beta diversity arose primarily from individual variation between enrichments rather than external*
136 *variables*

137 The taxa bar plots for the final time point indicated considerable variability in community
138 composition across the enrichments (Fig. 1A). We therefore performed additional analyses to
139 assess the impact of three external variables on beta diversity: time since inoculation, field site of
140 origin, and original sample type. PERMANOVA analysis indicated that time had a significant
141 effect on beta diversity regardless of whether ASV abundances and phylogenetic relationships
142 were accounted for (p = 0.001 for both Jaccard and weighted UniFrac distances) (Table 1).
143 However, the effect was relatively small (R^2 = 0.04 and 0.08 for Jaccard and weighted UniFrac
144 distances, respectively), and the respective PCoA plots suggested that the effect was not
145 particularly consistent over time or across different enrichments (Fig. 2A). Indeed, the time to
146 reach a stable community composition varied across the enrichments, with some appearing to
147 largely stabilize following the first 1:10 dilution transfer after week four; some experiencing
148 another dramatic shift following the second 1:10 dilution transfer after week eight; and a few
149 appearing to undergo a more or less continuous shift starting after the first transfer and continuing
150 to the end of the experiment (Fig. S1). Additionally, PERMDISP analysis indicated that the sample
151 dispersions differed significantly across different time points (p = 0.001 for both Jaccard and
152 weighted UniFrac distances) (Table 1), which can cause a significant PERMANOVA result even
153 if there is no difference in the group centroids.

154 The field site of origin (Biggs versus Staten Island) also had a statistically significant effect
155 on community composition (PERMANOVA p = 0.001 for both Jaccard and weighted UniFrac
156 distances, permuting only within each time point given the significant effect of time) (Table 1).
157 However, while the PCoA plot based on Jaccard distances revealed an almost perfect separation
158 between enrichments from the two fields, this was not evident with weighted UniFrac distances
159 (Fig. 2B), and the overall effect of field site was again quite small in both cases (R^2 = 0.05 and
160 0.03 for Jaccard and weighted UniFrac distances, respectively). Original sample type (rhizosphere,
161 root, or stem) also had a significant effect on community composition (PERMANOVA p = 0.001
162 for both Jaccard and weighted UniFrac distances, permuting only within each time point), with
163 slightly larger effect sizes compared to field site (R^2 = 0.07 and 0.13 for Jaccard and weighted
164 UniFrac distances, respectively). Indeed, while the PCoA plots suggested a high degree of overlap
165 among rhizosphere and root enrichments, the stem enrichments clustered separately to a moderate
166 degree based on both Jaccard and weighted UniFrac distances (Fig. 2C). However, PERMDISP
167 indicated that as with the effect of time, sample dispersions also differed for the two field sites and
168 across the different sample types (p = 0.001 for both Jaccard and weighted UniFrac distances)
169 (Table 1).
170 In contrast to the relatively small effects of the above variables, by far the greatest
171 proportion of the beta diversity was explained by individual enrichment identity, i.e. the unique
172 combination of field site, sample type, replicate, and dilution (PERMANOVA p = 0.001, R^2 = 0.44
173 for weighted UniFrac) (Table 1). The marginal effects of replicate and dilution were very small
174 (R^2 = 0.01 and 0.02 respectively), although still statistically significant (p = 0.001) (Table 1). We
175 therefore also asked whether enrichments derived from the same original sample but with different
176 inoculum dilutions ("within sample") ended up more similar to each other at the final time point

177 than enrichments derived from different original samples ("between sample"). In the case of
178 Jaccard distances (which take into account only the presence/absence of each ASV), there was a
179 statistically significant difference for the "within sample" versus "between sample" comparison
180 (Fig. 2D). This intuitively makes sense as enrichments derived from the same original sample
181 would be expected to share a higher proportion of ASVs, given the lack of opportunities for
182 dispersal between the enrichments over time. Notably, however, based on the weighted UniFrac
183 metric, which provides an arguably better representation of overall differences in community
184 structure, there was no statistically significant difference for "within sample" versus "between
185 sample" distances.

186 *Stochastic processes dominated the enrichment community assembly*

187 Given the high degree of variability in final community composition, even across
188 individual enrichments derived from the same original sample, we hypothesized that stochastic
189 processes had contributed significantly to community assembly in the enrichments. We therefore
190 sought to quantitatively infer the contribution of stochastic versus deterministic ecological
191 processes (i.e. drift versus selection), using two related statistical methods known as QPEN
192 ("Quantifying assembly Processes based on Entire-community Null model analysis") and iCAMP
193 ("infer Community Assembly Mechanisms by Phylogenetic-bin-based null model analysis") (20–
194 22). Both approaches are founded on the observation that more closely related species tend to
195 occupy more similar niches; thus, if the abundance-weighted phylogenetic relationships between
196 two communities' members are on average significantly closer than expected by chance given the
197 full set of taxa observed across all communities, this suggests that deterministic selection is at
198 work in similar environments. Consistent with our hypothesis, QPEN suggested that ecological
199 drift was the dominant process for 75% of all pairwise comparisons among the final enrichment

200 communities, while homogenous selection was the dominant ecological process for just 5%.
201 Similarly, iCAMP indicated that drift was the dominant process for the majority of phylogenetic
202 bins in 70% of the pairwise comparisons, while dispersal limitation and homogenous selection
203 were dominant in 8% and 5% of the comparisons respectively.

204 As an orthogonal approach to assess the potential contribution of deterministic forces to
205 the assembly of the enrichment communities, we performed consensus clustering analysis on the
206 final communities after collapsing the taxonomy abundance table to the family level. Consensus
207 clustering is a method of estimating how many subclasses (in this case, types of community
208 structures) are present in a dataset (23), and has previously been used to infer whether deterministic
209 forces contributed to variation across different enrichment communities (24). Specifically, if the
210 number of inferred community types is much less than the number of samples, this would suggest
211 some degree of determinism (non-randomness) in the community assembly process. Inspection of
212 the delta area plot (in which lower values represent lesser gains in cluster stability with increasing
213 *k*), as well as the cumulative distribution functions and heatmaps of the consensus matrices for
214 different *k*'s (numbers of clusters), suggested that the optimal number of clusters was 9 (Fig. 3A-
215 C, Fig. S2). However, clusters 5, 6, 7, and 9 were represented by only a single enrichment each.
216 Organizing the taxonomy abundance bar plots by cluster identity suggested that cluster 1 (the
217 largest cluster) was driven by a relatively high abundance of Methylocystaceae, whereas cluster 2
218 (the second-largest cluster) was driven by a high abundance of Comamonadaceae paired with a
219 lower abundance of Methylocystaceae (Fig. 3D). Cluster 3 was appeared to be driven by a high
220 abundance of ASVs that could not be classified beyond the domain Bacteria, cluster 4 was driven
221 by a high abundance of Methylococcaceae, and cluster 8 was driven by a high abundance of
222 Chromobacteriaceae. The samples in the four other clusters did not fall into any of these categories.

223 Taken together, these results suggest that despite the uniform culture conditions and
224 theoretically strong selective force imposed by the use of minimal media with methane as the only
225 added electron donor, stochastic processes (such as chance colonization—i.e. which strains were
226 present at time zero—and random extinction) were important drivers of community assembly in
227 our enrichments. Accordingly, even though certain types of community structures were more
228 prevalent than others among the final enrichments (as revealed by the consensus clustering
229 analysis), unpredictable and unique community structures also emerged.

230 *Putative parasitic bacteria belonging to the Candidate Phylum Radiation transiently bloomed in*
231 *multiple independent enrichments*

232 We were intrigued by the observation that ASVs that could not be classified beyond the
233 domain Bacteria were abundant in several of the enrichments. This was particularly striking in the
234 case of the final timepoint of the Staten Island root 2 10^{-2} enrichment, where the relative abundance
235 of a single unclassified bacterial sequence, ASV607, was 40.9%. Besides ASV607, five other
236 unclassified bacterial ASVs appeared at a relative abundance of >5% at least three times in our
237 enrichment time course dataset: ASV611, ASV616, ASV684, ASV697, and ASV891 (Fig. 4A). To
238 gain insight into the possible nature of these taxa, we used BLAST to search the respective ASV
239 sequences against the NCBI core nucleotide database (Table S3). For ASV697, the best named hit
240 was uncultured member of Chlamydiota detected in Chinese rice paddy soil, while for ASV684,
241 the best named hit was an uncultured member of Lentisphaerota detected in lake sediment (also
242 located in China), another environmental source of methane. For ASV616, there was no named hit
243 with coverage >50%, but the top overall hits were from environments such as subsurface water, a
244 sewage stabilization pond, and floodplain soil. For all three of the remaining sequences, the top
245 named hits belonged to the members of the Candidate Phylum Radiation (CPR)—specifically, the

246 candidate phyla Altimarinota (a.k.a. Gracilibacteria; ASV607 and ASV611) and
247 Peregrinibacteriota (ASV891). Notably, the top overall hit for ASV891 was a 100% match to an
248 unclassified 16S sequence from water that had been used to rinse rice grains; the second-best
249 overall hit for ASV607 was a 97.83% match to an unclassified 16S sequence from the "heavy"
250 isotopic fraction of activated sludge that had been incubated with ^{13}C-labeled methane; and the top
251 overall hits for ASV611 included sequences from lake sediment and a wetland. Taken together,
252 these results suggest that bacteria closely related to the unclassified sequences in our enrichments
253 might commonly occur in environments where methane is abundant.

254 Given that ASV607 was the most prevalent and abundant unclassified ASV in our
255 enrichments (Fig. 4A), we focused on this taxon for further analysis. Members of the CPR, to
256 which ASV607 putatively belongs, are mostly uncultivated but are thought to primarily be ultra-
257 small (~200-500 nm diameter) episymbiotic parasites of other bacteria (25, 26). To determine
258 whether such bacteria were present in a sample containing ASV607, we performed scanning
259 electron microscopy (SEM) on the Staten Island root 2 10^{-2} enrichment after regrowing it from a
260 frozen glycerol stock under the same conditions as the original enrichment; we focused on this
261 enrichment because it had the highest relative abundance of ASV607 at the end of the original time
262 course. Strikingly, we found multiple examples of such a bacterium in this culture: small (~340
263 nm diameter) cocci or diplococci that in all cases (n = 4) appeared to be directly attached to a larger
264 host (Fig. 4B). Although we cannot be sure that these bacteria represent ASV607, no other 16S
265 rRNA gene sequences belonging to the CPR or to other putative episymbionts were detected in the
266 original enrichment. Together, these observations lend credence to the possibility that ASV607 is
267 an episymbiont, similar to other studied members of the CPR.

268 Finally, we attempted to identify of the potential host(s) of ASV607 by looking for other
269 ASVs whose abundances were correlated with this taxon. Since ASV607 might by chance not
270 occur in every enrichment where its host was present, we first subsetted our enrichment time course
271 dataset to only the enrichments where ASV607 was detected at least once. We then used two
272 complementary methods of correlation analysis: SparCC, which was designed to handle some of
273 the challenging characteristics of microbiome data (e.g. compositionality and sparsity) (27), and
274 Pearson correlation, the method with the highest sensitivity for detecting parasitic interactions in
275 a prior study based on simulated data (28). Importantly, the latter study also demonstrated that
276 parasitic interactions between two taxa usually present as positive correlations (i.e. co-occurrence)
277 rather than negative correlations in microbial abundance data (28). Only two ASVs were
278 significantly positively correlated with ASV607 according to both methods: ASV7 (classified as
279 Methylophilaceae) and ASV441 (classified as Spartobacteria). When we highlighted the
280 abundances of these ASVs in the enrichments where ASV607 occurred, it became clear that
281 ASV607 occurred at relatively high abundances in multiple enrichments where ASV441 was
282 consistently below detection (Fig. 4C). By contrast, ASV7 was detected at least once in all of the
283 enrichments where ASV607 was abundant, and at many timepoints these two taxa co-occurred
284 with similar relative abundances (Fig. 4C). Thus, although we currently cannot rule out the
285 possibility that ASV441 (or other taxa) could be a host for ASV607, ASV7 (Methylophilaceae)
286 appears to be the most likely candidate for the primary host.

287 *Strains from the enrichments possess variable repertoires for metabolism of carbon and nitrogen*

288 Given that the enrichment cultures were fed only with methane, the abundance and
289 diversity of non-methanotrophic strains raised the question of what carbon sources could be
290 supporting their growth. Methanotrophic activity has been shown to contribute to the pool of

291 organic acids in rice paddy soils (12). Additionally, it has been previously reported that some
292 methanotrophs can cross-feed methanol (the first product of methane oxidation) to non-
293 methanotrophic methylotrophs (29). We therefore investigated whether organic acids and/or
294 methanol could plausibly support the growth of members of the enrichment communities.

295 To do so, we isolated a total of 64 strains from the enrichments (Table S4). Of these isolates,
296 three are methanotrophs (*Methylosinus* DMC42, *Methylosinus* DMC45, and *Methylocystis*
297 DMC101), while the rest are non-methane-utilizing heterotrophs. The isolates represent 12 of the
298 16 families that had reached a final relative abundance of >10% in at least two enrichments
299 (missing representatives only for Verrucomicrobiaceae, Methylococcaceae, Bradyrhizobiaceae,
300 and Prolixibacteraceae). Three isolates belonging to the genus *Methyloraptor*, in the family
301 Ancalomicrobiaceae, matched a similarly prevalent and abundant ASV that had been classified
302 only to order level as Rhizobiales. We also obtained isolates for several other families that were
303 less prevalent and/or abundant in the final enrichments, including Moraxellaceae,
304 Sphingomonadaceae, Xanthobacteraceae, Caulobacteraceae, Devosiaceae, Microbacteriaceae,
305 Sphaerotilaceae, and additional members of Rhizobiaceae (one of which had dominated a Biggs
306 stem enrichment).

307 To obtain strain-level insights into the potential catabolic capabilities of the enrichment
308 community members, we generated draft genome assemblies for a diverse selection of isolates
309 representing most of the families in our collection. We then assessed the non-methanotrophic
310 isolates' genomic potential for the consumption of 62 common carbon sources, using the program
311 GapMind (30). We considered a strain likely to be able to use a carbon source if GapMind
312 identified a complete pathway with only high-confidence hits, and a "maybe" if GapMind
313 identified a complete pathway but at least one step was at best a medium-confidence hit. Strains

314 were considered unlikely to be able to use a carbon source if any of the best hits in the respective
315 pathway were low-confidence, i.e. "gaps." This analysis revealed that nearly all of the sequenced
316 isolates are likely to be able to use fumarate as a carbon source, and most of the isolates (with the
317 exception of members of Methylophilaceae and *Cloacibacterium*) are also likely to be able to use
318 multiple other organic acids, such as succinate, malate, and acetate (Fig. 5; Table S5). By
319 comparison, the capacity to utilize sugar-related compounds and amino acids as carbon sources
320 appeared to be less widespread.

321 We also assessed whether the non-methanotrophic isolates could potentially utilize
322 methanol, which is not included in GapMind. To do so, we searched the genomes for homologs of
323 the four known types of methanol dehydrogenases (calcium-dependent Mxa; lanthanide-
324 dependent Xox; the type I alcohol dehydrogenase Mdh2; and NAD-dependent Mdh) (Fig. 6A;
325 Table S5). For strains that possessed at least one putative methanol dehydrogenase, we also looked
326 for homologs of the genes needed for the ribulose monophosphate (RuMP) cycle, the serine cycle,
327 and the Calvin cycle, which are the three known pathways for assimilation of C1 units by
328 methylotrophic bacteria (31) (Fig. 6B; Table S5). The results were mostly consistent with what has
329 been reported for the respective taxonomic groups: members of *Methylovorus*, *Methylophilus*,
330 *Methylobacterium*, *Methyloraptor, Oharaeibacter*, and *Xanthobacter* are all known methylotrophs,
331 and all sequenced isolates from these genera possessed both Mxa and Xox, as well as a complete
332 C1 assimilation pathway. However, one isolate from a genus not known to be methylotrophic also
333 showed possible genomic capacity for methylotrophy: *Pinisolibacter* sp. DMC19 possesses a
334 homolog of XoxF (though it seemingly lacks other Xox genes), as well as a complete Calvin cycle.
335 Another *Pinisolibacter* isolate also possesses XoxF and a near-complete Calvin cycle, but appears
336 to be missing glyceraldehyde-3-phosphate dehydrogenase; while *Oryzibacter oryziterrae* DMC98

337 possesses XoxF along with a near-complete serine cycle, but appears to be missing
338 phosphoenolpyruvate carboxylase. A few other isolates from genera not typically known to
339 consume methanol contained putative homologs of XoxF, Mdh2, and/or NAD-dependent Mdh,
340 but lacked multiple steps in each of the C1 assimilation pathways, suggesting that they are unlikely
341 to use methanol as a carbon source.

342 Finally, given that methanotrophic activity has previously been shown to impact nitrogen
343 cycling in rice paddy soils (12, 17), we assessed the genomic capacity for each isolate, including
344 methanotrophs, to fix nitrogen and/or perform denitrification. Several strains possessed *nifD*, *nifK*,
345 and *nifH*, indicating that they can likely fix nitrogen (Fig. 7; Table S5); these belonged to the genera
346 *Pseudacidovorax*, *Burkholderia*, *Xanthobacter*, *Aquabacter*, *Pinisolibacter*, *Methyloraptor*,
347 *Methylophilus*, and *Methylosinus* (which is methanotrophic). Among these, to our knowledge the
348 nitrogen-fixing potential of *Pinisolibacter* and *Methylophilus* has not been previously reported
349 (although a metagenome-assembled genome classified under the family Methylophilaceae, to
350 which *Methylophilus* belongs, was recently found to contain a *nif* locus (32)). Only two out of
351 three sequenced isolates of *Methylophilus* possessed the *nif* genes, indicating that nitrogen fixing
352 capabilities vary within this genus. As for denitrification potential, we found a variety of
353 combinations of genes involved in the different steps of denitrification (Fig. 7; Table S5). Only
354 *Pinisolibacter* sp. DMC100 possessed a complete denitrification pathway. Some strains appeared
355 to be capable of only nitrate reduction; others only had the genes for nitrous oxide reduction. Still
356 others lacked the genes for nitrate reduction but possessed all other steps of denitrification, or
357 conversely had all steps except for nitrous oxide reduction. Additionally, three strains only
358 possessed the genes for non-consecutive steps (nitrate and nitric oxide reduction, nitrate and
359 nitrous oxide reduction, or nitrite and nitrous oxide reduction).

360

361 **Discussion**

362 In this study, we utilized methane-fed enrichment cultures to determine which bacterial
363 members of the rice microbiota can be supported by methane-derived carbon, revealing
364 considerable taxonomic diversity among the potential beneficiaries of methanotrophic activity. We
365 found that the composition of rice-derived, methane-supported microbial communities is
366 significantly affected by the type of plant part used as the inoculum (with stem enrichments
367 exhibiting lower alpha diversity than root and rhizosphere enrichments), but is less affected by
368 field site (Fig. 2, Table 1). The lower alpha diversity of the stem enrichments is consistent with
369 prior studies indicating that the stem or leaf microbiotas of rice and other plants tend to have lower
370 alpha diversity compared to the rhizosphere and roots (33, 34). While many of our enrichments
371 had a high abundance of type II methanotrophs and/or members of Comamonadaceae, a variety of
372 overall community structures emerged (Fig. 1, Fig. 3), suggesting a limited contribution of
373 deterministic forces to community assembly during growth on methane. Finally, genomic analysis
374 indicated that organic acids and methanol are likely carbon sources that may support the growth
375 of many non-methanotrophs in methane-fed communities (Fig. 5, Fig. 6). Taken together, these
376 results shed new light on the contribution of methanotrophs to the rice microbiome.

377 The diversity of non-methanotrophic taxa that were enriched alongside methanotrophs in
378 our cultures, representing at least 14 families, greatly expands the knowledge of which taxa may
379 benefit from methanotrophic activity in rice paddies. In prior DNA-SIP studies where rice roots or
380 paddy soils were incubated with isotopically-labeled methane, relatively few taxa were identified
381 (10–12), possibly due to the limited sensitivity of this technique and the presence of alternative
382 carbon sources in those experimental setups. In our enrichments, as in the DNA-SIP studies, some

383 carbon from the soil or plant material would have been present at the start of the experiment, but
384 any such nutrients would have then been diluted by the two sequential transfers, if not already fully
385 consumed in the first few weeks of incubation. Thus, with the possible exception of a few
386 enrichments where the final abundance of putative methanotrophs appeared to be extremely low
387 (which may have occurred due to stochastic extinction), taxa that were abundant at the final
388 timepoint of our enrichments were likely primarily supported by methane-derived carbon. Among
389 the non-methanotrophic taxonomic groups that were particularly prevalent and/or abundant in our
390 enrichments, Comamonadaceae, Methylophilaceae, Rhizobiales, and Sphingomonadales have also
391 been labeled with methane-derived carbon in DNA-SIP studies (10, 12), providing further
392 evidence that these taxa genuinely benefit from methanotrophic activity in rice fields.

393 The heterogeneity of our enrichments indicated a significant contribution of stochastic
394 ecological forces to community assembly during growth under methane. While this may in part
395 have been driven by the particulars of our experimental setup (e.g., the use of a dilution series, and
396 the relatively long four-week incubation time between transfers), the variety of observed
397 community structures, together with the diversity of the enriched taxa, suggests that the impact of
398 altering methanotrophic activity in rice microbiomes might not be easily predicted. That being said,
399 our enrichments also bore some taxonomic resemblance to previous studies on methane-supported
400 microbial communities from other environments. For example, *Methylophilus*, *Pseudomonas*, and
401 *Flavobacterium*, three prominent genera in our enrichments (Fig. 1), were also prevalent in
402 methane-fed enrichments from lake sediment (35, 36). Moreover, a study on naturally-occurring
403 methane-supported biofilms in a mineral spring cave reported the presence of Flavobacteriales,
404 Verrucomicrobia, Rhizobiales, Sphingomonadales, Pseudomonadales, and Xanthomonodales,
405 among other non-methanotrophic taxa (37), all of which were abundant in at least two of our

406 enrichments (note that Verrucomicrobia also encompasses methanotrophic acidophiles belonging
407 to the genera *Methylacidiphilum* and *Methylacidimicrobium* (38), but these were not detected in
408 either the mineral spring cave or our enrichments). Thus, it appears that the assembly of methane-
409 supported communities is not entirely random, and many of the taxonomic groups in our
410 enrichments may be associated with methanotrophs not only in rice paddies, but also more broadly.
411 Another notable finding was the prevalence of CPR bacteria in our enrichments (Fig. 4,
412 Table S3). To our knowledge, this phenomenon has not previously been explicitly reported in a
413 methane-supported microbial ecosystem. However, many of the closest sequenced relatives for the
414 putative CPR bacteria in our enrichments were also derived from environments where methane is
415 abundant, indicating that our detection of CPR members in methanotrophic communities is not an
416 anomaly. Given that the DNA of one such organism was labeled with methane-derived carbon in
417 a DNA-SIP study (see Table S3), some of these bacteria may be genuine beneficiaries of the
418 activity of methanotrophs. This interpretation is further supported by the positive correlation
419 between ASV607 (a putative CPR member) and ASV7 (a member of the methylotrophic family
420 *Methylophilaceae*) in our enrichments (Fig. 4C). Importantly, standard 16S primer pairs are a poor
421 match for many CPR members (39). Thus, these organisms may be even more prevalent and
422 abundant in rice microbiomes and other methane-supported microbial communities than is
423 reflected in currently available data. Detailed studies on CPR bacteria are challenging due to the
424 difficulty of isolating these organisms. Nevertheless, future attempts to confirm the identity of the
425 host(s) for rice-associated CPR bacteria, and to ascertain the nature of the host-epibiont
426 relationship (parasitic, predatory, or commensal), may help improve the understanding of rice
427 microbiome dynamics.

428 Regarding the question of how non-methanotrophic growth is supported in methane-fed
429 communities, the prevalence of pathways for organic acid catabolism in isolates from our
430 enrichments (Fig. 5) is consistent with the idea that organic acids are likely a key class of cross-
431 fed metabolites, corroborating prior evidence that methanotrophs contribute to organic acid
432 production in paddy soils (12). Whether this contribution is primarily direct or indirect remains
433 unclear, but certain type I and type II methanotrophs have been shown to excrete organic acids in
434 pure cultures during growth on methane under low oxygen conditions (40–42). Low oxygen
435 conditions likely prevailed in our enrichment cultures over time, as the initial molar ratio of oxygen
436 to methane in the headspace was less than 1 (see Materials and Methods), whereas two oxygen
437 molecules are required to oxidize one molecule of methane all the way to carbon dioxide (43).
438 Additionally, the abundance of several methylotrophic taxa in our enrichments (Fig. 1, Fig. 6)
439 suggests that methanol may also have been cross-fed from methanotrophs, as has been previously
440 demonstrated in pairwise co-cultures of a methanotroph and a methylotroph (29). However,
441 organic acids and methanol may not be the only cross-fed carbon sources in methanotroph-
442 supported communities. Several taxa enriched in our cultures belong to the phylum Bacteroidota,
443 members of which are best known for their ability to degrade complex carbohydrates (44).
444 Consequently, it has previously been suggested that Bacteroidota members that frequently co-
445 occur with methanotrophs (e.g., *Flavobacterium* species) may be supported by extracellular
446 polysaccharides produced by other community members, though direct evidence of such
447 interactions is still lacking (5). These taxa proved difficult to isolate from our enrichments, and
448 thus we only have one representative genome sequence so far, from a strain of *Cloacibacterium*.
449 Potentially consistent with the extracellular polysaccharide hypothesis, this strain does not possess
450 high-confidence pathways for the usage of either organic acids or methanol (Fig. 5), suggesting

451 that it may indeed have been supported by other compounds in the enrichment cultures. We also
452 cannot rule out that nutrients may also have been released by cell lysis over the course of our
453 experiment, potentially supporting some of the taxa that only persisted at a very low relative
454 abundance in the enrichments. While beyond the scope of the current study, future work will be
455 directed at more precisely identifying the carbon sources exchanged among members of
456 methanotroph-supported microbial communities.

457 Finally, the presence of genes related to nitrogen cycling in the majority of isolates from
458 the enrichments is consistent with previous indications of functional links between methanotrophy,
459 nitrogen fixation, and denitrification in rice paddy microbial communities (12, 45). Whether the
460 activity of methanotrophs tends to stimulate nitrogen fixation or denitrification more strongly *in*
461 *situ* is unknown; the balance between the two presumably depends not only on the makeup of a
462 given community, but also environmental parameters such as local oxygen gradients and
463 application of fertilizers (45, 46). With respect to denitrification, we observed that many strains
464 possessed only partial pathways (Fig. 7), as is common in many natural environments (47),
465 suggesting that cross-feeding of not only carbon sources (electron donors) but also denitrification
466 intermediates (electron acceptors) may occur in methanotroph-supported communities under low
467 oxygen tensions. As mentioned above, oxygen tension was likely low in our enrichments for much
468 of the time course, making nitrate an important alternative electron acceptor that could have shaped
469 the emergent community structures.

470 In summary, our findings suggest that methanotrophs can help support a wide range of
471 metabolically-diverse heterotrophic bacteria in the microbial ecosystem of rice paddies, with the
472 potential for impacts on important ecosystem functions such as nitrogen fixation and
473 denitrification. Furthermore, our collection of 64 taxonomically-diverse isolates, more than half of

which have draft genomes, represents a valuable resource for future mechanistic studies on how rice-associated methanotrophs interact with their native neighbors. Given that methanotrophs affect both carbon cycling and nitrogen cycling in rice paddies, it will be worthwhile to continue gaining a deeper understanding of how methanotrophic bacteria influence the structure and function of the rice microbiome under different conditions, so as to support the long-term sustainability and productivity of this globally-important staple crop.

Acknowledgements

This work was supported by the Laboratory Directed Research & Development program at Lawrence Berkeley National Laboratory [award number 23-071 to D.C.]. We thank the Sundaresan and Schuppenhauer labs for providing the field-grown rice plants, Deepika Awasthi for assistance with establishing a methane gassing station, Morgan Price for assistance with data processing, and Misun Kang and the staff at the University of California Berkeley Electron Microscope Laboratory for advice and assistance with electron microscopy sample preparation and imaging.

Materials and Methods

Time course of methane-fed enrichment cultures

Six rice plants were collected from two fields (three plants per field), located in Biggs, California (39.4643, -121.7340) and Staten Island, California (38.1235, -121.5490), in the summer of 2022. The Biggs samples were collected in late July, and the Staten Island samples were collected in late August. Each plant was collected from a different area of the respective field and had the entire root structure dug up with the attached soil. The collected plants were placed in

497 individual clean zipper-top plastic bags in 5-gallon buckets and transported back to the laboratory.
498 The protocol for establishing methane-fed cultures from the rhizosphere was based on previous
499 work (48), with modifications made to include the root and stem. For each plant, after removing
500 soil not tightly bound to roots, a portion of the roots was dissected and placed in a 15 mL conical
501 tube containing 10 mL of dilute nitrate mineral salts (dNMS) media, made according to the recipe
502 of (48) except that the vitamin solution was procured from the American Type Culture Collection
503 (catalog no. MD-VS). The complete media composition is provided in Table S6. The roots were
504 vigorously vortexed to generate the rhizosphere samples. Then, a portion of the roots was ground
505 in 1 mL dNMS for 45 s using a sterilized stainless-steel grinding jar (Qiagen, catalog no. 69985)
506 in a Qiagen TissueLyser II. Stem samples were processed in a similar manner. 0.5 mL of the
507 homogenized samples, representing the week 0 time point, was spun down at 4000 rpm for 20 min
508 in a tabletop centrifuge, and the pellets were stored at -20°C until DNA extraction. The remainder
509 of each sample was diluted 10^{-2}, 10^{-3}, and 10^{-4} in dNMS (Staten Island stem samples were only
510 diluted up to 10^{-3}), and 0.5 mL of the resulting suspensions was injected into sealed, autoclaved
511 Balch tubes containing 5 mL of dNMS. Approximately 5 mL of the headspace was removed by
512 syringe and replaced with 5 mL of methane to create a 20% methane headspace. The cultures were
513 incubated upright with shaking at 24°C. Every seven days, 0.5 mL was collected from each culture
514 and pelleted for later DNA extraction as above. Additionally, 70 µL of each culture was used to
515 make a frozen stock in 15% glycerol, stored at -80°C. At the same time, 5 mL of headspace was
516 withdrawn and replaced with another 5 mL of methane. Every four weeks, 0.5 mL of each culture
517 was transferred to a new Balch tube containing 5 mL of fresh dNMS. The experiment was
518 terminated after a total of 12 weeks. Note that in this setup, the cultures were most likely electron
519 acceptor-limited rather than methane-limited. The initial quantities of methane and oxygen per

520 tube were 210 µmol and 140 µmol respectively, whereas two moles of oxygen are required to
521 completely oxidize one mole of methane to carbon dioxide (43), involving the transfer of 8 electron
522 equivalents (dioxygen can accept 4 electron equivalents per mole). Even if nitrate was used as an
523 alternative electron acceptor by some community members, only 12.5 µmol of nitrate was supplied
524 (which can accept 5 electron equivalents per mole via complete denitrification).

525 *16S rRNA gene amplicon sequencing*

526 Genomic DNA was extracted from pelleted samples using the Qiagen DNeasy Blood &
527 Tissue kit (catalog no. 69506), following the manufacturer's protocol for Gram-positive bacteria.
528 The extracted DNA was PCR amplified using dual-index 16S V4-V5 primers (515F/926R) (49).
529 A peptide nucleic acid (PNA) PCR clamp was used to block the amplification of plastid and
530 mitochondrial DNA (50). The resulting libraries were quantified using the Qubit dsDNA BR Assay
531 kit (Invitrogen, catalog no. Q32853), pooled, cleaned using a PCR purification kit, and sequenced
532 on an Illumina MiSeq (PE 2x300). The paired-end reads were assembled using PEAR (51), and
533 reads with more than one expected error were detected using USEARCH (52) and discarded, along
534 with rare sequences (fewer than 4 reads in any sample). Chimera removal and error correction
535 were performed with the UNOISE3 algorithm (53). Taxonomy was assigned using SINTAX (54)
536 with the RDP training set v18.

537 *16S sequencing data analysis*

538 The following initial analysis steps were performed in Qiime2 (version amplicon-2024.5):
539 Samples were rarefied to 900 reads (based on the histogram of reads per sample), a phylogenetic
540 tree was constructed using MAFFT alignment and FastTree, core alpha and beta diversity metrics
541 were calculated, and principal coordinate analysis (PCoA) matrices were generated. SparCC and
542 Pearson correlation analyses were also performed in Qiime2, using the SCNIC plugin (55). All

543 other analyses were performed in R. PERMANOVA analyses were performed with the adonis2
544 function from the package vegan (version 2.6-10) (56). PERMDISP tests were performed with the
545 permutest function in conjunction with the betadisper function, also from vegan. When testing the
546 effect of time point, permutations were constrained within each enrichment and the data were
547 treated as a series. When testing the effect of field site or sample type, permutations were
548 constrained within time point. Assessment of the contribution of stochastic versus deterministic
549 processes during community assembly was performed using the functions qpen and icamp.big in
550 the iCAMP package (20). Consensus clustering was performed using the package
551 ConsensusClusterPlus, with maxK = 17, reps = 100, pItem = 0.8, pFeature = 1, and clusterAlg =
552 "hc" (57). Except for the consensus clustering plots, which were produced by the
553 ConsensusClusterPlus package, all plots were made with the R package ggplot2 (58).

554 *Scanning electron microscopy*

555 To prepare the scanning electron microscopy (SEM) sample (Electron Microscopy
556 Laboratory, University of California, Berkeley), the Staten Island root 2 10^{-2} enrichment was
557 regrown, from a frozen glycerol stock, in dNMS with 20% methane (shaking at 125 rpm at 25°C).
558 The regrown culture was sub-cultured twice at a 1:100 dilution ratio on day 15 and day 23. On day
559 29, 10 mL of the culture was pelleted (5000 g for 10 min), and the cells were gently resuspended
560 in a fixative solution (2% glutaraldehyde in 0.1M sodium cacodylate buffer, pH 7.2). The sample
561 was placed at 4°C on a rotator overnight and subsequently stored at 4°C in the dark (standing) until
562 further processing. Prior to imaging, the sample was washed 3x in 0.1M sodium cacodylate buffer,
563 pH 7.2, postfixed 3x in 1% osmium tetroxide in 0.1M sodium cacodylate buffer, pH 7.2 for 1 h,
564 and then washed 3x in 0.1M sodium cacodylate buffer, pH 7.2. Samples were dehydrated in a
565 graded ethanol series up to 100%. Samples were then transferred onto 0.1% (w/v) poly-L-lysine–

566 coated coverslips and subjected to critical point drying (Tousimis, Mayland, USA). The dried
567 coverslips were mounted onto aluminum stubs using conductive carbon tape and sputter-coated
568 with a gold/palladium alloy (Safematic GmbH, Switzerland). SEM imaging was performed using
569 a Zeiss Crossbeam 550 (Carl Zeiss Microsystems GmbH, Oberkochen, Germany).

570 *Isolation of strains from the enrichment cultures*

571 Strains were isolated from the original enrichment cultures, as well as enrichments regrown
572 from frozen glycerol stocks, by plating a 10-fold dilution series onto dNMS with 1.5% agarose
573 and 0.2% methanol; dNMS agarose under a mixed methane/air atmosphere; or 0.1x R2A with 1.5%
574 agar. To obtain the *Methylocystis* isolate, a 10-fold dilution series (10^{-1} to 10^{-8}) of an enrichment
575 regrown from the frozen stock was set up in a 48-well plate and incubated statically under 20%
576 methane at room temperature for 4 weeks; then, a loopful of the culture in the 10^{-8} dilution well
577 was streaked onto dNMS agarose and incubated under a mixed methane/air atmosphere. The mixed
578 methane/air atmosphere was achieved by flooding a mostly-closed BD EZ Incubator Container
579 with methane for 30-60s and then quickly latching the lid. All plates were incubated at room
580 temperature, and morphologically distinct colonies were picked and restreaked 3-4 times until the
581 colony morphologies appeared uniform. The 16S rRNA gene was then amplified by colony PCR,
582 using Platinum Hot Start Master Mix (Invitrogen) with the primers 27F
583 (AGAGTTTGATCMTGGCTCAG) and 1492R (TACGGYTACCTTGTTACGACTT). The PCR
584 products were Sanger sequenced at Elim Biopharm, Inc. with the same 27F and 1492R primers.
585 The resulting forward and reverse sequences were aligned in Geneious Prime and subjected to
586 BLAST against the NCBI core nucleotide database.

587 *Genomic analysis of isolated strains*

588 Genomic DNA was isolated from selected strains using the Qiagen DNeasy Blood & Tissue
589 kit (catalog no. 69506), following the manufacturer's protocol for Gram-positive bacteria. Library
590 preparation and whole-genome sequencing was performed by Novogene on an Illumina NovaSeq
591 X Plus. The raw reads were cleaned with Trimmomatic on KBase (59), using the default settings.
592 Draft genomes were assembled with SPAdes (v3.15.3), with the minimum contig size set to 1000
593 bp, and annotated with Prokka (v1.145), also on KBase. Genomes were checked for completeness
594 and contamination with CheckM. Taxonomy was assigned using the Microbial Genomes Atlas
595 pipeline against the Genome Taxonomy Database (GTDB, version r214) (60, 61). Annotation of
596 common carbon source utilization pathways was performed using the online GapMind tool (30).
597 Detection of homologs of known methanol dehydrogenases was performed using DIAMOND with
598 the "sensitive" setting (62); a hit was considered a homolog if it had >40% identity to the reference
599 sequence, with at least 80% coverage. The list of reference methanol dehydrogenase sequences
600 was obtained from a prior publication (63). For C1 assimilation pathways, DIAMOND with the
601 same settings failed to detect complete pathways in some of the known methylotrophs. We
602 therefore instead used HMMER (version 3.4) (64) with the HMM profiles from the same prior
603 publication (63), requiring hits to have at least 80% coverage of the respective model to be
604 considered a homolog. Genes related to nitrogen cycling were detected using the application
605 "Search with HMMs of MicroTrait Bioelement families - v1" on KBase (59, 65).

606 *Data availability*

607 The raw sequence data for 16S rRNA gene amplicons from the enrichments are available on the
608 NCBI Sequence Read Archive (SRA) under the accession PRJNA1310742. Draft genome
609 assemblies have been deposited DDBJ/ENA/GenBank under the accession PRJNA1310743.

610

611 **References**

612

613 1. Hanson RS, Hanson TE. 1996. Methanotrophic bacteria. Microbiol Rev 60:439–471.

614 2. Auman AJ, Speake CC, Lidstrom ME. 2001. nifH Sequences and Nitrogen Fixation in Type

615 I and Type II Methanotrophs. Appl Environ Microbiol 67:4009–4016.

616 3. Eisentraeger A, Klag P, Vansbotter B, Heymann E, Dott W. 2001. Denitrification of

617 groundwater with methane as sole hydrogen donor. Water Research 35:2261–2267.

618 4. Knowles R. 2005. Denitrifiers associated with methanotrophs and their potential impact on

619 the nitrogen cycle. Ecological Engineering 24:441–446.

620 5. Chistoserdova L, Kalyuzhnaya MG. 2018. Current Trends in Methylotrophy. Trends in

621 Microbiology 26:703–714.

622 6. Whittenbury R, Phillips KC, Wilkinson JF. 1970. Enrichment, Isolation and Some

623 Properties of Methane-utilizing Bacteria. Journal of General Microbiology 61:205–218.

624 7. Ho A, De Roy K, Thas O, De Neve J, Hoefman S, Vandamme P, Heylen K, Boon N. 2014.

625 The more, the merrier: heterotroph richness stimulates methanotrophic activity. The ISME

626 Journal 8:1945–1948.

627 8. Stock M, Hoefman S, Kerckhof F-M, Boon N, De Vos P, De Baets B, Heylen K, Waegeman

628 W. 2013. Exploration and prediction of interactions between methanotrophs and

629 heterotrophs. Research in Microbiology 164:1045–1054.

630 9. Iguchi H, Yurimoto H, Sakai Y. 2011. Stimulation of Methanotrophic Growth in Cocultures

631 by Cobalamin Excreted by Rhizobia. Appl Environ Microbiol 77:8509–8515.

632 10. Qiu Q, Conrad R, Lu Y. 2009. Cross-feeding of methane carbon among bacteria on rice

633 roots revealed by DNA-stable isotope probing. Environ Microbiol Rep 1:355–361.

634 11. Murase J, Frenzel P. 2007. A methane-driven microbial food web in a wetland rice soil.
635 Environmental Microbiology 9:3025–3034.
636 12. Chen K-H, Feng J, Bodelier PLE, Yang Z, Huang Q, Delgado-Baquerizo M, Cai P, Tan W,
637 Liu Y-R. 2024. Metabolic coupling between soil aerobic methanotrophs and denitrifiers in
638 rice paddy fields. Nat Commun 15:3471.
639 13. Osaka T, Ebie Y, Tsuneda S, Inamori Y. 2008. Identification of the bacterial community
640 involved in methane-dependent denitrification in activated sludge using DNA stable-isotope
641 probing: Characterization of a MDD ecosystem by SIP. FEMS Microbiology Ecology
642 64:494–506.
643 14. Dumont MG, Pommerenke B, Casper P, Conrad R. 2011. DNA-, rRNA- and mRNA-based
644 stable isotope probing of aerobic methanotrophs in lake sediment. Environmental
645 Microbiology 13:1153–1167.
646 15. Hutchens E, Radajewski S, Dumont MG, McDonald IR, Murrell JC. 2004. Analysis of
647 methanotrophic bacteria in Movile Cave by stable isotope probing. Environmental
648 Microbiology 6:111–120.
649 16. Bridgham SD, Cadillo-Quiroz H, Keller JK, Zhuang Q. 2013. Methane emissions from
650 wetlands: biogeochemical, microbial, and modeling perspectives from local to global
651 scales. Global Change Biology 19:1325–1346.
652 17. Cao W, Cai Y, Bao Z, Wang S, Yan X, Jia Z. 2022. Methanotrophy Alleviates Nitrogen
653 Constraint of Carbon Turnover by Rice Root-Associated Microbiomes. Front Microbiol
654 13:885087.

655 18. Muthayya S, Sugimoto JD, Montgomery S, Maberly GF. 2014. An overview of global rice
656 production, supply, trade, and consumption. Annals of the New York Academy of Sciences
657 1324:7–14.
658 19. Neufeld JD, Dumont MG, Vohra J, Murrell JC. 2007. Methodological Considerations for
659 the Use of Stable Isotope Probing in Microbial Ecology. Microbial Ecology 53:435–442.
660 20. Ning D, Yuan M, Wu L, Zhang Y, Guo X, Zhou X, Yang Y, Arkin AP, Firestone MK, Zhou
661 J. 2020. A quantitative framework reveals ecological drivers of grassland microbial
662 community assembly in response to warming. Nat Commun 11:4717.
663 21. Stegen JC, Lin X, Fredrickson JK, Chen X, Kennedy DW, Murray CJ, Rockhold ML,
664 Konopka A. 2013. Quantifying community assembly processes and identifying features that
665 impose them. The ISME Journal 7:2069–2079.
666 22. Stegen JC, Lin X, Fredrickson JK, Konopka AE. 2015. Estimating and mapping ecological
667 processes influencing microbial community assembly. Front Microbiol 6:370.
668 23. Monti S, Tamayo P, Mesirov J, Golub T. 2003. Consensus Clustering: A Resampling-Based
669 Method for Class Discovery and Visualization of Gene Expression Microarray Data.
670 Machine Learning 52:91–118.
671 24. Celiker H, Gore J. 2014. Clustering in community structure across replicate ecosystems
672 following a long-term bacterial evolution experiment. Nat Commun 5:4643.
673 25. Méheust R, Burstein D, Castelle CJ, Banfield JF. 2019. The distinction of CPR bacteria
674 from other bacteria based on protein family content. Nat Commun 10:4173.
675 26. Ji Y, Zhang P, Zhou S, Gao P, Wang B, Jiang J. 2022. Widespread but Poorly Understood
676 Bacteria: Candidate Phyla Radiation. Microorganisms 10:2232.

677 27. Friedman J, Alm EJ. 2012. Inferring Correlation Networks from Genomic Survey Data.
678 PLOS Computational Biology 8:e1002687.
679 28. Weiss S, Van Treuren W, Lozupone C, Faust K, Friedman J, Deng Y, Xia LC, Xu ZZ, Ursell
680 L, Alm EJ, Birmingham A, Cram JA, Fuhrman JA, Raes J, Sun F, Zhou J, Knight R. 2016.
681 Correlation detection strategies in microbial data sets vary widely in sensitivity and
682 precision. ISME J 10:1669–1681.
683 29. Krause SMB, Johnson T, Samadhi Karunaratne Y, Fu Y, Beck DAC, Chistoserdova L,
684 Lidstrom ME. 2017. Lanthanide-dependent cross-feeding of methane-derived carbon is
685 linked by microbial community interactions. Proc Natl Acad Sci USA 114:358–363.
686 30. Price MN, Deutschbauer AM, Arkin AP. 2022. Filling gaps in bacterial catabolic pathways
687 with computation and high-throughput genetics. PLoS Genet 18:e1010156.
688 31. Chistoserdova L. 2011. Modularity of methylotrophy, revisited. Environmental
689 Microbiology 13:2603–2622.
690 32. Yu L, Jia R, Liu S, Li S, Zhong S, Liu G, Zeng RJ, Rensing C, Zhou S. 2024. Ferrihydrite-
691 mediated methanotrophic nitrogen fixation in paddy soil under hypoxia. ISME
692 Communications 4:ycae030.
693 33. Wagner MR, Lundberg DS, del Rio TG, Tringe SG, Dangl JL, Mitchell-Olds T. 2016. Host
694 genotype and age shape the leaf and root microbiomes of a wild perennial plant. Nat
695 Commun 7:12151.
696 34. Zhang X, Ma Y-N, Wang X, Liao K, He S, Zhao X, Guo H, Zhao D, Wei H-L. 2022.
697 Dynamics of rice microbiomes reveal core vertically transmitted seed endophytes.
698 Microbiome 10:216.

699 35. Oshkin IY, Beck DAC, Lamb AE, Tchesnokova V, Benuska G, McTaggart TL,
700 Kalyuzhnaya MG, Dedysh SN, Lidstrom ME, Chistoserdova L. 2015. Methane-fed
701 microbial microcosms show differential community dynamics and pinpoint taxa involved in
702 communal response. The ISME Journal 9:1119–1129.
703 36. Van Grinsven S, Sinninghe Damsté JS, Harrison J, Polerecky L, Villanueva L. 2021. Nitrate
704 promotes the transfer of methane-derived carbon from the methanotroph *Methylobacter* sp.
705 to the methylotroph *Methylotenera* sp. in eutrophic lake water. Limnology & Oceanography
706 66:878–891.
707 37. Karwautz C, Kus G, Stöckl M, Neu TR, Lueders T. 2018. Microbial megacities fueled by
708 methane oxidation in a mineral spring cave. The ISME Journal 12:87–100.
709 38. Schmitz RA, Peeters SH, Versantvoort W, Picone N, Pol A, Jetten MSM, Op den Camp
710 HJM. 2021. Verrucomicrobial methanotrophs: ecophysiology of metabolically versatile
711 acidophiles. FEMS Microbiol Rev 45:fuab007.
712 39. Brown CT, Hug LA, Thomas BC, Sharon I, Castelle CJ, Singh A, Wilkins MJ, Wrighton
713 KC, Williams KH, Banfield JF. 2015. Unusual biology across a group comprising more
714 than 15% of domain Bacteria. Nature 523:208–211.
715 40. Vecherskaya M, Dijkema C, Saad HR, Stams AJM. 2009. Microaerobic and anaerobic
716 metabolism of a Methylocystis parvus strain isolated from a denitrifying bioreactor.
717 Environmental Microbiology Reports 1:442–449.
718 41. Tays C, Guarnieri MT, Sauvageau D, Stein LY. 2018. Combined effects of carbon and
719 nitrogen source to optimize growth of proteobacterial methanotrophs. Front Microbiol
720 9:2239.

721 42. Kalyuzhnaya MG, Yang S, Rozova ON, Smalley NE, Clubb J, Lamb A, Gowda GAN,
722 Raftery D, Fu Y, Bringel F, Vuilleumier S, Beck DAC, Trotsenko YA, Khmelenina VN,
723 Lidstrom ME. 2013. Highly efficient methane biocatalysis revealed in a methanotrophic
724 bacterium. Nat Commun 4:2785.
725 43. Reis PCJ, Tsuji JM, Weiblen C, Schiff SL, Scott M, Stein LY, Neufeld JD. 2024. Enigmatic
726 persistence of aerobic methanotrophs in oxygen-limiting freshwater habitats. The ISME
727 Journal 18:wrae041.
728 44. Gavriilidou A, Gutleben J, Versluis D, Forgiarini F, van Passel MWJ, Ingham CJ, Smidt H,
729 Sipkema D. 2020. Comparative genomic analysis of Flavobacteriaceae: insights into
730 carbohydrate metabolism, gliding motility and secondary metabolite biosynthesis. BMC
731 Genomics 21:569.
732 45. Cao W, Cai Y, Bao Z, Wang S, Yan X, Jia Z. 2022. Methanotrophy Alleviates Nitrogen
733 Constraint of Carbon Turnover by Rice Root-Associated Microbiomes. Front Microbiol 13.
734 46. Ishii S, Ikeda S, Minamisawa K, Senoo K. 2011. Nitrogen Cycling in Rice Paddy
735 Environments: Past Achievements and Future Challenges. Microbes and Environments
736 26:282–292.
737 47. Roothans N, van Loosdrecht MCM, Laureni M. 2025. Metabolic labour division trade-offs
738 in denitrifying microbiomes. The ISME Journal 19:wraf020.
739 48. Rahalkar MC, Khatri K, Pandit P, Bahulikar RA, Mohite JA. 2021. Cultivation of Important
740 Methanotrophs From Indian Rice Fields. Front Microbiol 12:669244.
741 49. Thompson LR, Sanders JG, McDonald D, Amir A, Ladau J, Locey KJ, Prill RJ, Tripathi A,
742 Gibbons SM, Ackermann G, Navas-Molina JA, Janssen S, Kopylova E, Vázquez-Baeza Y,
743 González A, Morton JT, Mirarab S, Zech Xu Z, Jiang L, Haroon MF, Kanbar J, Zhu Q, Jin

744 Song S, Kosciolek T, Bokulich NA, Lefler J, Brislawn CJ, Humphrey G, Owens SM,
745 Hampton-Marcell J, Berg-Lyons D, McKenzie V, Fierer N, Fuhrman JA, Clauset A, Stevens
746 RL, Shade A, Pollard KS, Goodwin KD, Jansson JK, Gilbert JA, Knight R. 2017. A
747 communal catalogue reveals Earth's multiscale microbial diversity. Nature 551:457–463.
748 50. Lundberg DS, Yourstone S, Mieczkowski P, Jones CD, Dangl JL. 2013. Practical
749 innovations for high-throughput amplicon sequencing. Nat Methods 10:999–1002.
750 51. Zhang J, Kobert K, Flouri T, Stamatakis A. 2014. PEAR: a fast and accurate Illumina
751 Paired-End reAd mergeR. Bioinformatics 30:614–620.
752 52. Edgar RC. Search and clustering orders of magnitude faster than BLAST.
753 53. Edgar RC. 2016. UNOISE2: improved error-correction for Illumina 16S and ITS amplicon
754 sequencing. bioRxiv https://doi.org/10.1101/081257.
755 54. Edgar RC. 2016. SINTAX: a simple non-Bayesian taxonomy classifier for 16S and ITS
756 sequences. bioRxiv https://doi.org/10.1101/074161.
757 55. Shaffer M, Thurimella K, Sterrett JD, Lozupone CA. 2023. SCNIC: Sparse correlation
758 network investigation for compositional data. Molecular Ecology Resources 23:312–325.
759 56. Oksanen J, Simpson GL, Blanchet FG, Kindt R, Legendre P, Minchin PR, O'Hara RB,
760 Solymos P, Stevens MHH, Szoecs E, Wagner H, Barbour M, Bedward M, Bolker B,
761 Borcard D, Borman T, Carvalho G, Chirico M, Caceres MD, Durand S, Evangelista HBA,
762 FitzJohn R, Friendly M, Furneaux B, Hannigan G, Hill MO, Lahti L, Martino C, McGlinn
763 D, Ouellette M-H, Cunha ER, Smith T, Stier A, Braak CJFT, Weedon J. 2025. vegan:
764 Community Ecology Package (2.6-10).
765 57. Wilkerson MD, Hayes DN. 2010. ConsensusClusterPlus: a class discovery tool with
766 confidence assessments and item tracking. Bioinformatics 26:1572–1573.

767 58. Wickham H. 2016. ggplot2: Elegant Graphics for Data Analysis. Springer-Verlag New
768 York. https://ggplot2.tidyverse.org.
769 59. Arkin AP, Cottingham RW, Henry CS, Harris NL, Stevens RL, Maslov S, Dehal P, Ware D,
770 Perez F, Canon S, Sneddon MW, Henderson ML, Riehl WJ, Murphy-Olson D, Chan SY,
771 Kamimura RT, Kumari S, Drake MM, Brettin TS, Glass EM, Chivian D, Gunter D, Weston
772 DJ, Allen BH, Baumohl J, Best AA, Bowen B, Brenner SE, Bun CC, Chandonia J-M, Chia
773 J-M, Colasanti R, Conrad N, Davis JJ, Davison BH, DeJongh M, Devoid S, Dietrich E,
774 Dubchak I, Edirisinghe JN, Fang G, Faria JP, Frybarger PM, Gerlach W, Gerstein M,
775 Greiner A, Gurtowski J, Haun HL, He F, Jain R, Joachimiak MP, Keegan KP, Kondo S,
776 Kumar V, Land ML, Meyer F, Mills M, Novichkov PS, Oh T, Olsen GJ, Olson R, Parrello
777 B, Pasternak S, Pearson E, Poon SS, Price GA, Ramakrishnan S, Ranjan P, Ronald PC,
778 Schatz MC, Seaver SMD, Shukla M, Sutormin RA, Syed MH, Thomason J, Tintle NL,
779 Wang D, Xia F, Yoo H, Yoo S, Yu D. 2018. KBase: The United States Department of
780 Energy Systems Biology Knowledgebase. Nat Biotechnol 36:566–569.
781 60. Parks DH, Chuvochina M, Rinke C, Mussig AJ, Chaumeil P-A, Hugenholtz P. GTDB: an
782 ongoing census of bacterial and archaeal diversity through a phylogenetically consistent,
783 rank normalized and complete genome-based taxonomy.
784 61. Rodriguez-R LM, Gunturu S, Harvey WT, Rosselló-Mora R, Tiedje JM, Cole JR,
785 Konstantinidis KT. 2018. The Microbial Genomes Atlas (MiGA) webserver: taxonomic and
786 gene diversity analysis of Archaea and Bacteria at the whole genome level. Nucleic Acids
787 Res 46:W282–W288.
788 62. Buchfink B, Xie C, Huson DH. 2015. Fast and sensitive protein alignment using
789 DIAMOND. Nat Methods 12:59–60.

790 63. Salcher MM, Schaefle D, Kaspar M, Neuenschwander SM, Ghai R. 2019. Evolution in
791 action: habitat transition from sediment to the pelagial leads to genome streamlining in
792 Methylophilaceae. ISME J 13:2764–2777.
793 64. Eddy SR. 2011. Accelerated Profile HMM Searches. PLOS Computational Biology
794 7:e1002195.
795 65. Karaoz U, Brodie EL. 2022. microTrait: A Toolset for a Trait-Based Representation of
796 Microbial Genomes. Front Bioinform 2.
797

798

Figures and Figure Legends

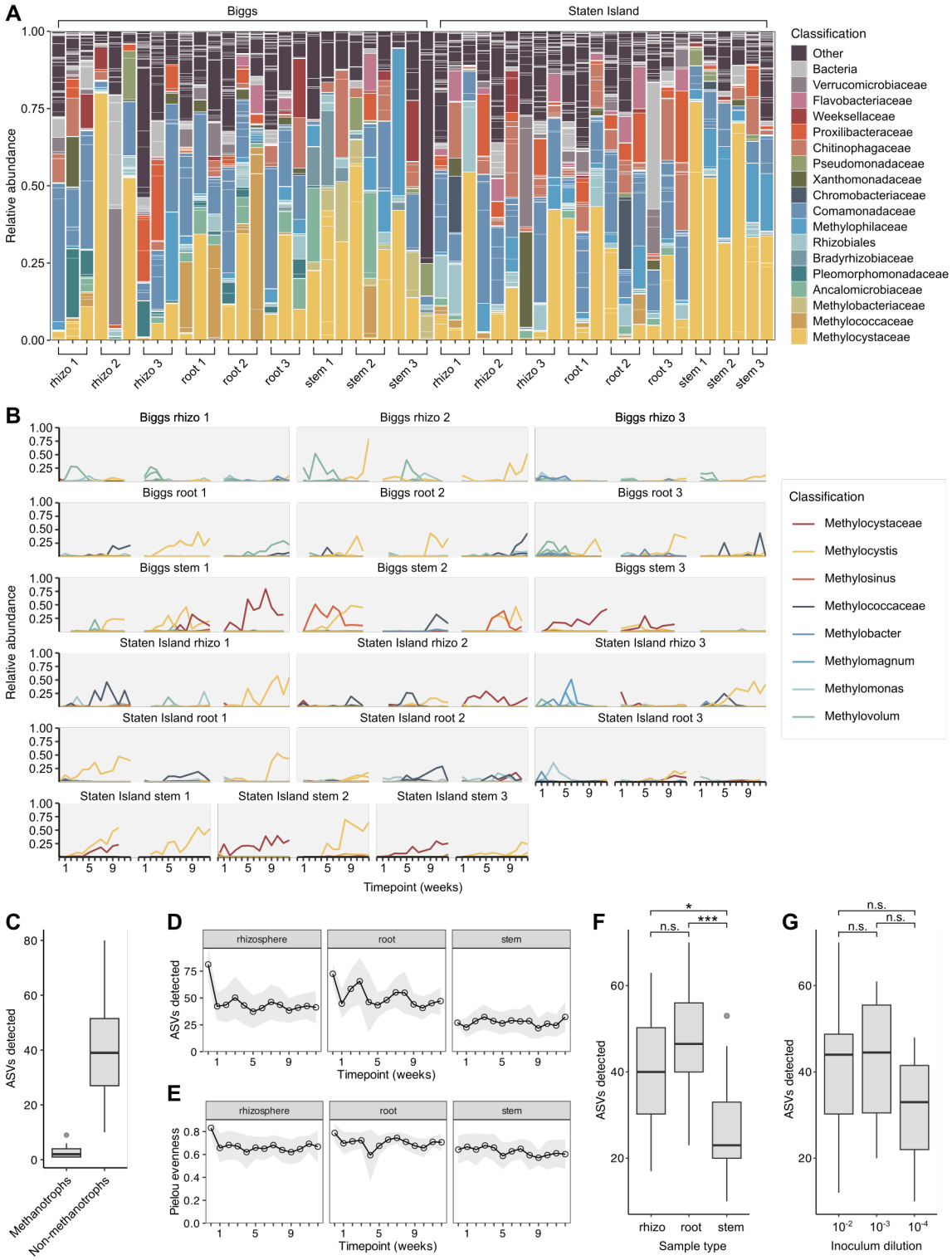

801 **Figure 1. Taxonomic diversity and dynamics of methane-fed enrichment cultures. A)** Taxa
802 bar plot showing the overall diversity and major families in the enrichment cultures at the final
803 sequenced timepoint. Individual ASVs within each family are separated by white lines. **B)**
804 Relative abundance of putative methanotroph ASVs over time in each enrichment. Under each
805 header (e.g. "Biggs rhizo 1"), the enrichments are arranged from left to right in order of
806 increasing inoculum dilution (i.e., 10^{-2}, 10^{-3}, 10^{-4}). **C)** The number of detected ASVs that were
807 classified as methanotrophs or non-methanotrophs in each enrichment at the final timepoint. **D-**
808 **E)** The number of ASVs detected (D) or Pielou evenness (E) of the enrichments over time,
809 separated by sample type. **F)** The number of ASVs detected in the enrichments at the final
810 timepoint, separated by sample type or by inoculum dilution. * $p < 0.05$, *** $p < 0.001$, ANOVA
811 followed by Tukey HSD.

812

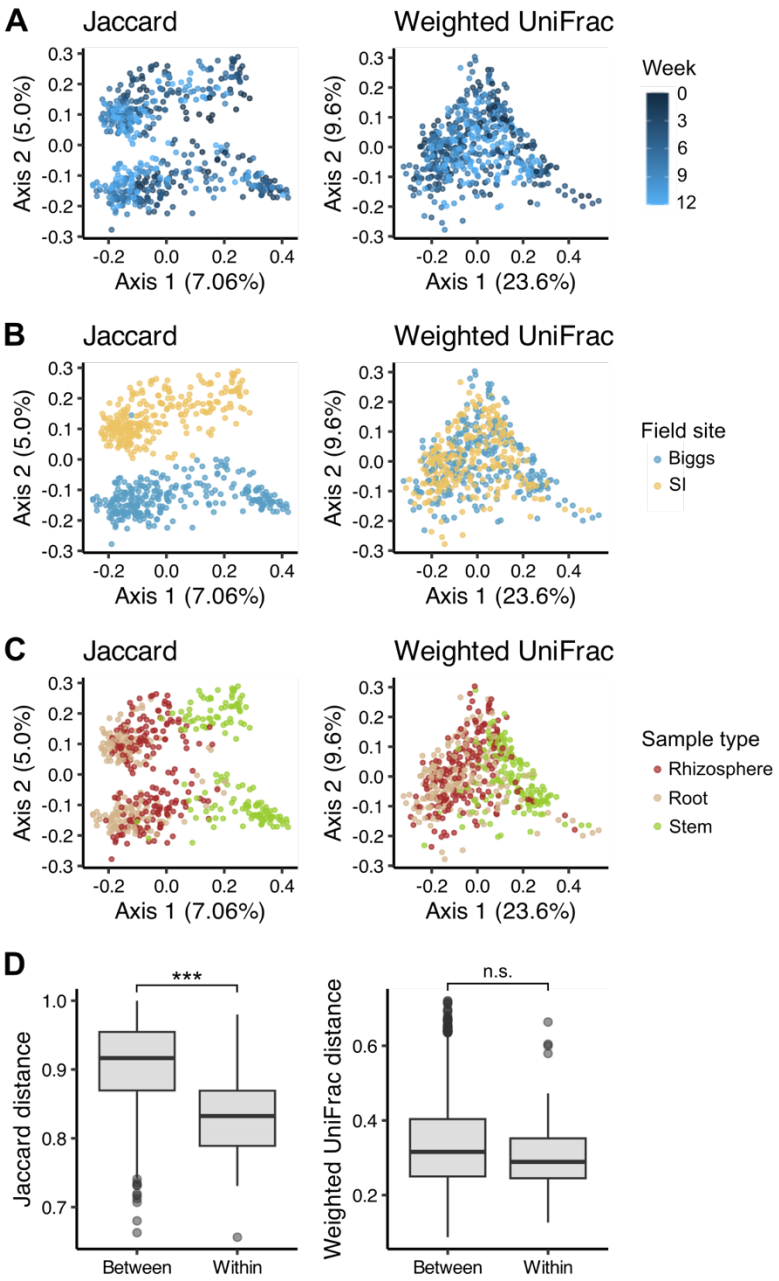

Figure 2. Impact of external variables on enrichment community beta diversity. A) PCoA plots of all sequenced enrichment samples, colored by time point. **B)** The same plots as in (A), but colored by field site. **C)** The same plots as in (A), but colored by sample type. **D)** Jaccard and weighted UniFrac distances for enrichments inoculated from different replicate plant parts

818 (“between”) versus enrichments inoculated from the same replicate plant part (albeit at different

819 dilutions; “within”).

820

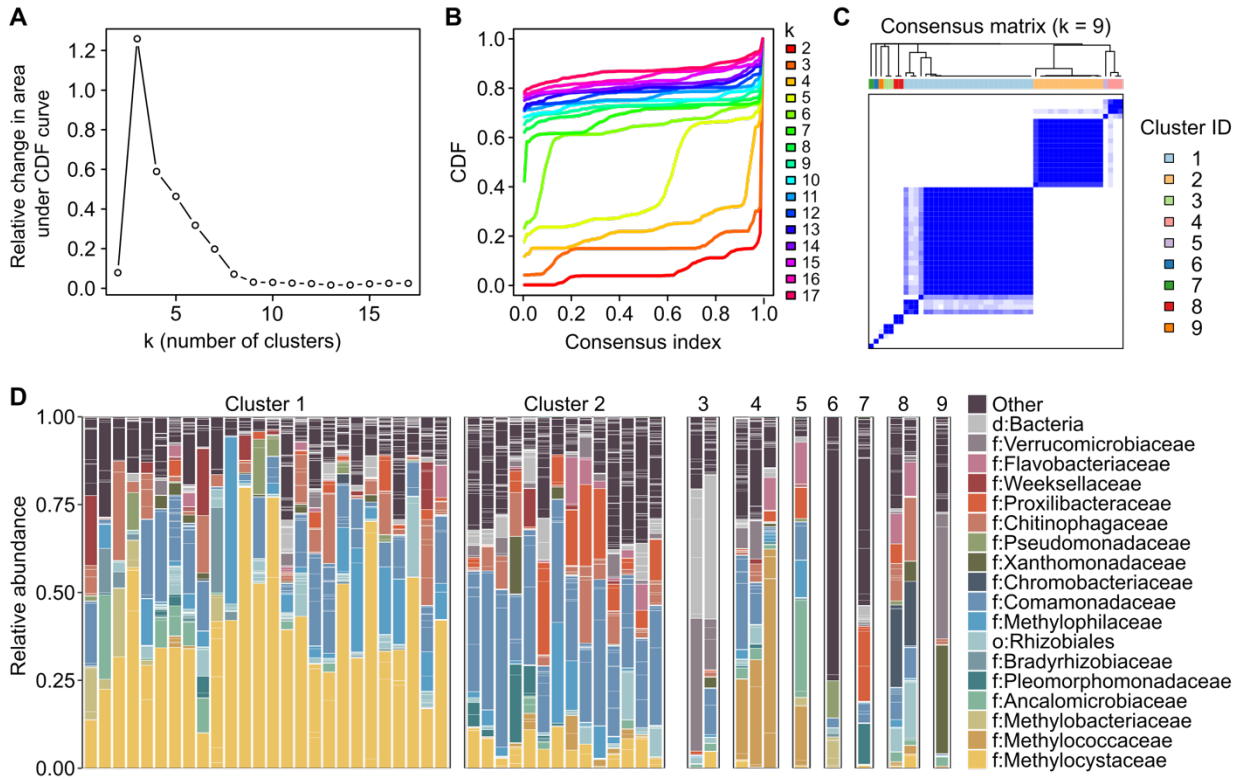

Figure 3. Consensus clustering analysis of enrichment communities. A) Delta area plot showing the relative change in area under the cumulative distribution function (CDF) curve for k versus $k - 1$. The optimal number of clusters is usually considered to be the value of k at which there is no longer an appreciable increase in area under the CDF. **B)** The CDFs of the consensus matrix for each k (indicated by colors), estimated by a histogram of 100 bins. **C)** The consensus matrix for $k = 9$. Darker blues in the matrix indicate higher consensus. **D)** Taxa bar plots for the samples in each consensus cluster for $k = 9$.

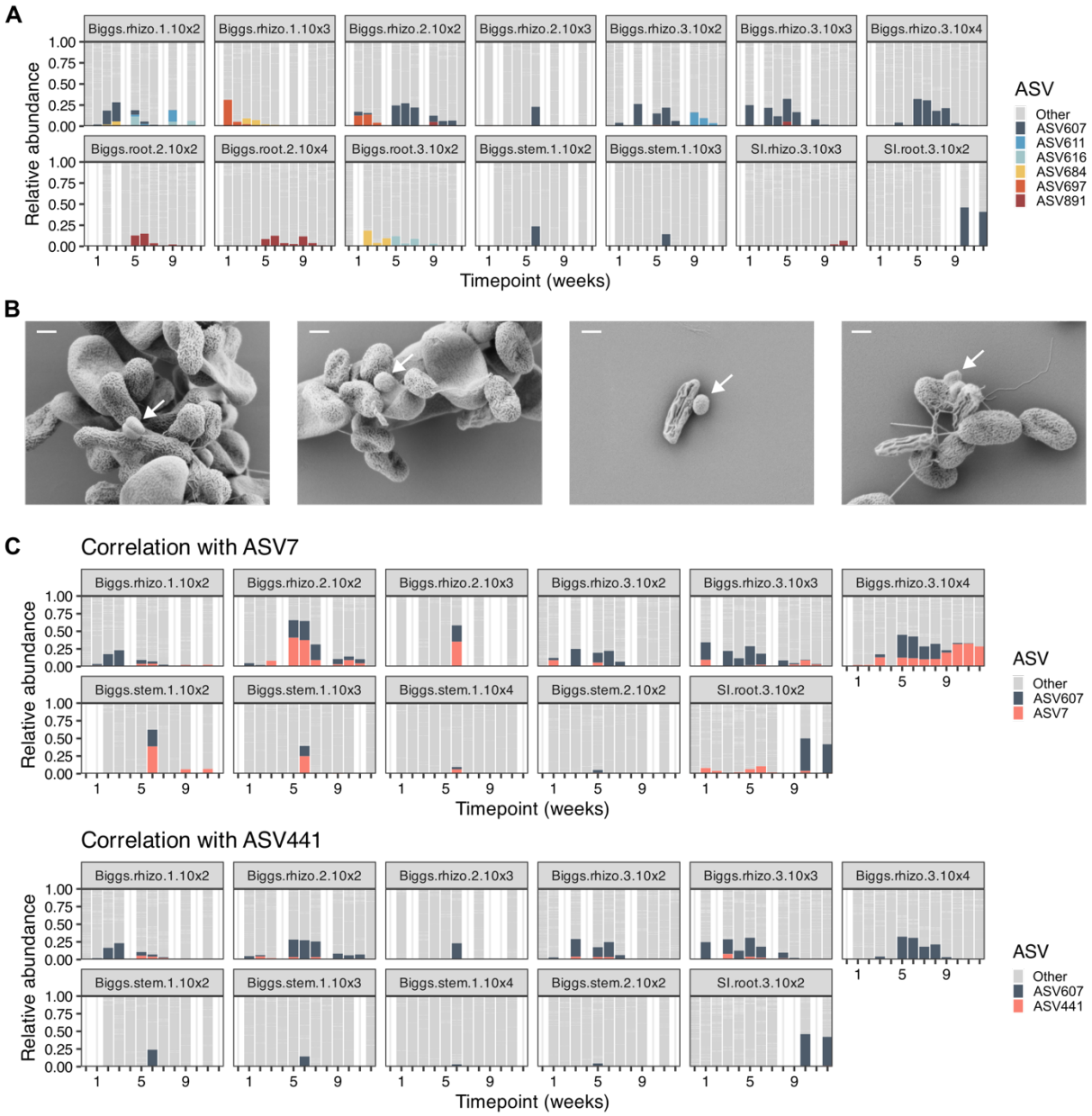

Figure 4. Presence of CPR bacteria in methane-fed enrichments. A) Taxa bar plot highlighting the six unclassified bacterial ASVs that appeared at a relative abundance of >5% at least three times (whether in different enrichments or multiple timepoints of a single enrichment). **B)** SEM images showing the putative CPR epibiont, marked with a white arrow.

835 Scale bar = 300 nm. **C)** Taxa bar plots highlighting ASV607 along with the two candidates for its

836 host based on correlation analysis.

837

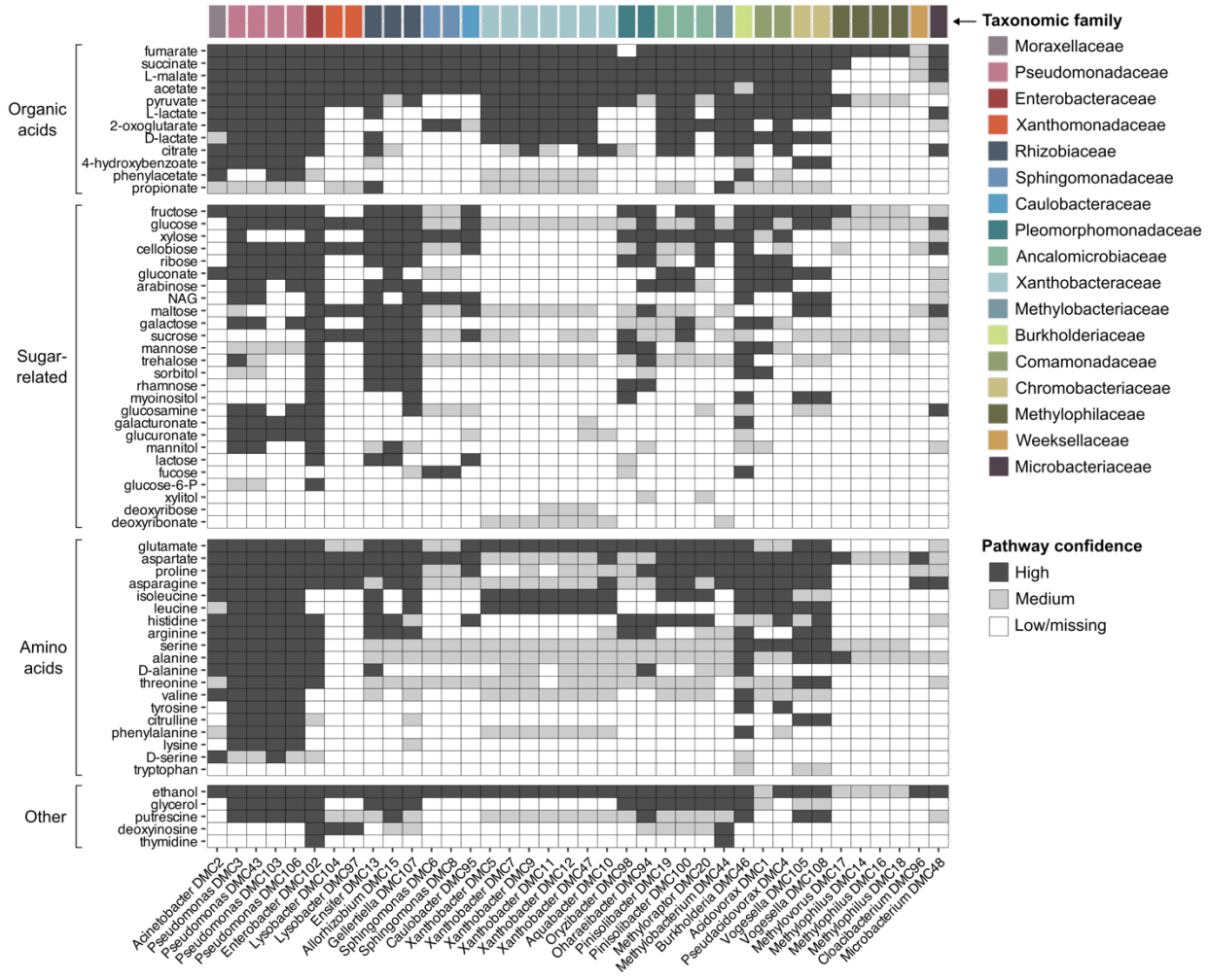

Figure 5. Putative carbon source utilization pathways in non-methanotrophic isolates from methane-fed enrichments. The presence of pathways for utilizing 62 common carbon sources was assessed for 38 isolate genomes using GapMind. Pathways were considered high, medium, or low confidence/missing according to the lowest confidence level for any step in the pathway (e.g. a pathway in which only a low-confidence hit was found for at least one step was considered low confidence overall).

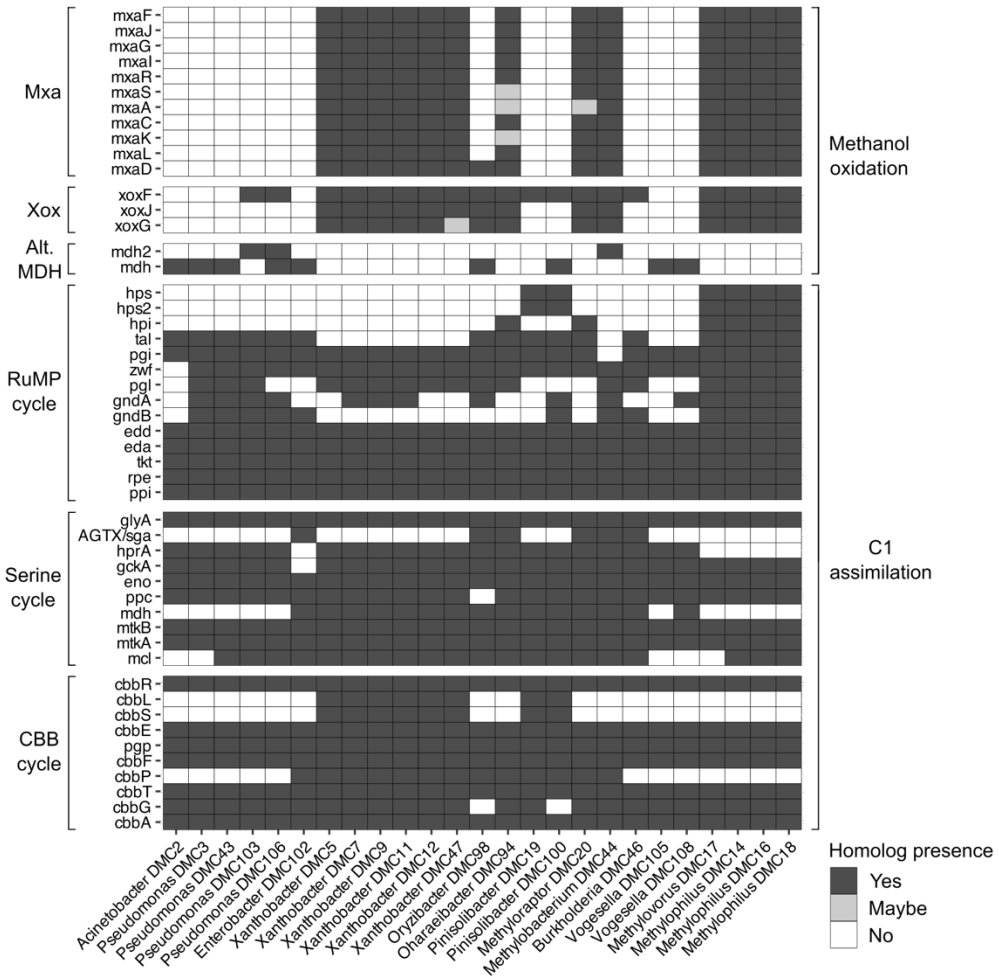

Figure 6. Genomic capacity for methanol catabolism in non-methanotrophic isolates from methane-fed enrichments. Presence of homologs of known methanol dehydrogenases and the genes needed for the three known bacterial C1 assimilation pathways. "Alt. MDH" = alternative methanol dehydrogenase other than the classical Mxa and Xox types. Only strains possessing at least one putative methanol dehydrogenase are shown. Homologs were detected using DIAMOND for methanol dehydrogenases (cutoffs: >40% identity and >80% coverage, with "maybe" denoting a hit with 37-39% ID and >80% coverage, or >40% identity and 75-79% coverage), and HMMER for C1 assimilation genes (cutoffs: e-value < 10^{-5} and coverage >80%).

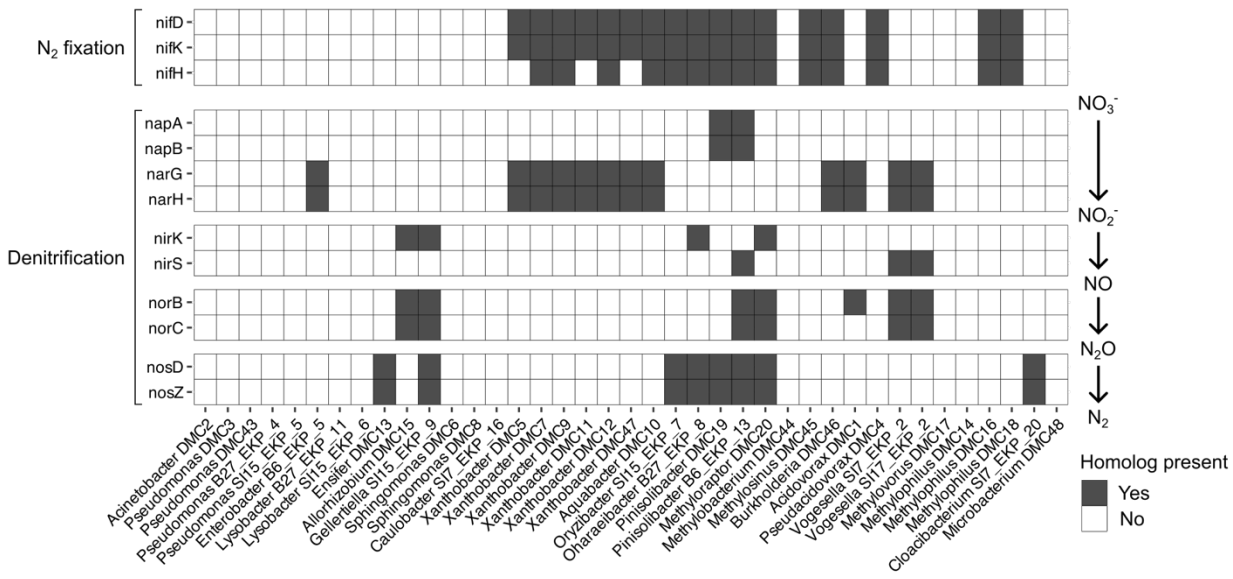

Figure 7. Genomic capacity for nitrogen fixation and denitrification in isolates from methane-fed enrichments. Presence of homologs of key genes needed for nitrogen fixation and the four steps of denitrification. Homologs were detected using microTrait on KBase. Nap and Nar are alternative nitrate reductases—i.e. only one of the two is needed to reduce nitrate to nitrite. Similarly, for reduction of nitrite to nitric oxide, either NirK or NirS is sufficient.

863 **Table 1. PERMANOVA and PERMDISP statistical test results.**

Distance metric	Test	Independent variable	R^2	Pseudo-F	Pr(>F)
Jaccard	PERMANOVA	Timepoint	0.04	2.0427	0.001
Weighted UniFrac	PERMANOVA	Timepoint	0.08	3.8124	0.001
Jaccard	PERMDISP	Timepoint	NA	5.8664	0.001
Weighted UniFrac	PERMDISP	Timepoint	NA	8.0389	0.001
Jaccard	PERMANOVA	Field site	0.05	25.623	0.001
Weighted UniFrac	PERMANOVA	Field site	0.03	14.035	0.001
Jaccard	PERMDISP	Field site	NA	50.335	0.001
Weighted UniFrac	PERMDISP	Field site	NA	19.947	0.001
Jaccard	PERMANOVA	Sample type	0.07	20.108	0.001
Weighted UniFrac	PERMANOVA	Sample type	0.13	39.414	0.001
Jaccard	PERMDISP	Sample type	NA	51.113	0.001
Weighted UniFrac	PERMDISP	Sample type	NA	17.582	0.001
Jaccard	PERMANOVA	Enrichment ID	0.52	10.412	0.001
Weighted UniFrac	PERMANOVA	Enrichment ID	0.44	7.4642	0.001
Jaccard	PERMANOVA	Replicate (marginal effect*)	0.01	7.9084	0.001
Weighted UniFrac	PERMANOVA	Replicate (marginal effect*)	0.01	7.9996	0.001
Jaccard	PERMANOVA	Dilution (marginal effect*)	0.02	6.1119	0.001
Weighted UniFrac	PERMANOVA	Dilution (marginal effect*)	0.02	7.8126	0.001

864 *Marginal effect indicates the effect of the term after taking into account all other terms in the
865 model (the terms were timepoint, field site, sample type, replicate, and dilution).

866